Free Radical Biology and Medicine 60 (2013) 282–291

Contents lists available at SciVerse ScienceDirect

Free Radical Biology and Medicine

journal homepage: www.elsevier.com/locate/freeradbiomed

Original Contrbution

Induction of oxidative and nitrosative damage leads to cerebrovascular inflammation in an animal model of mild traumatic brain injury induced by primary blast

P.M. Abdul-Muneer [a], Heather Schuetz [a], Fang Wang [c], Maciej Skotak [c], Joselyn Jones [b], Santhi Gorantla [a], Matthew C. Zimmerman [b], Namas Chandra [c], James Haorah [a,*]

[a] Department of Pharmacology and Experimental Neuroscience, University of Nebraska Medical Center, Omaha, NE 68198, USA
[b] Department of Cellular and Integrative Physiology, University of Nebraska Medical Center, Omaha, NE 68198, USA
[c] Department of Mechanical and Materials Engineering, University of Nebraska at Lincoln, Lincoln, NE 68588, USA

ARTICLE INFO

Article history:
Received 10 August 2012
Received in revised form
10 January 2013
Accepted 23 February 2013
Available online 4 March 2013

Keywords:
Mild traumatic brain injury
Blood–brain barrier
Oxidative stress
Perivascular unit
Neuroinflammation
Primary blast
Free radicals

ABSTRACT

We investigate the hypothesis that oxidative damage of the cerebral vascular barrier interface (the blood–brain barrier, BBB) causes the development of mild traumatic brain injury (TBI) during a primary blast-wave spectrum. The underlying biochemical and cellular mechanisms of this vascular layer-structure injury are examined in a novel animal model of shock tube. We first established that low-frequency (123 kPa) single or repeated shock wave causes BBB/brain injury through biochemical activation by an acute mechanical force that occurs 6–24 h after the exposure. This biochemical damage of the cerebral vasculature is initiated by the induction of the free radical-generating enzymes NADPH oxidase 1 and inducible nitric oxide synthase. Induction of these enzymes by shock-wave exposure paralleled the signatures of oxidative and nitrosative damage (4-HNE/3-NT) and reduction of the BBB tight-junction (TJ) proteins occludin, claudin-5, and zonula occluden 1 in the brain microvessels. In parallel with TJ protein disruption, the perivascular unit was significantly diminished by single or repeated shock-wave exposure coinciding with the kinetic profile. Loosening of the vasculature and perivascular unit was mediated by oxidative stress-induced activation of matrix metalloproteinases and fluid channel aquaporin-4, promoting vascular fluid cavitation/edema, enhanced leakiness of the BBB, and progression of neuroinflammation. The BBB leakiness and neuroinflammation were functionally demonstrated in an in vivo model by enhanced permeativity of Evans blue and sodium fluorescein low-molecular-weight tracers and the infiltration of immune cells across the BBB. The detection of brain cell proteins neuron-specific enolase and S100β in the blood samples validated the neuroastroglial injury in shock-wave TBI. Our hypothesis that cerebral vascular injury occurs before the development of neurological disorders in mild TBI was further confirmed by the activation of caspase-3 and cell apoptosis mostly around the perivascular region. Thus, induction of oxidative stress and activation of matrix metalloproteinases by shock wave underlie the mechanisms of cerebral vascular BBB leakage and neuroinflammation.

Published by Elsevier Inc.

Introduction

Traumatic brain injury (TBI) is characterized by physical brain injury as a result of acceleration–deceleration, resulting frequently from impact with an immobile object, that often leads to cognitive deficits and impairment of behavior. Unlike casualties suffered from moderate to severe TBI, victims diagnosed with mild TBI (mTBI) remain conscious, and typical symptoms include headache, confusion, dizziness, memory impairment, and behavioral changes. U.S. soldiers exposed to blast-wave pressure and combat experiences without any physical brain injury during Middle East wars are commonly diagnosed with mild TBI and posttraumatic stress disorder [1]. Mild TBI is the most frequent form of trauma among deployed military populations [2]. In recent military conflicts, the repeated exposure to low levels of blast overpressure from improvised explosive devices is believed to account for the majority of the mTBI's. Ironically, most of these soldiers exposed to low-intensity blast remain conscious, and many of these soldiers are frequently redeployed in the war zone without proper diagnosis. This in turn puts these military personnel in danger of experiencing consecutive multiple blast exposures aggravating an already existing medical condition [3,4]. These subjects undergo severe mental stress and often become misusers of alcohol and other drugs of abuse [5,6], and thereby the chances of mental health complications such as

* Corresponding author. Fax: +402 559 8922.
E-mail address: jhaorah@unmc.edu (J. Haorah).

0891-5849/$ - see front matter Published by Elsevier Inc.
http://dx.doi.org/10.1016/j.freeradbiomed.2013.02.029

posttraumatic stress disorder (PTSD) increase in the long term [7]. It seems that there is a strong overlap between symptoms of chronic mTBI and PTSD among many veterans reexposed to multiple blasts of wave pressure, which has become a major challenge for the military healthcare system. Psychological and physiological stress by repeated blast-wave exposure is believed to contribute significantly to the development of PTSD in chronic mTBI, resulting in alterations in cognitive behaviors [4,8]. These findings are further supported by recent demonstration in an animal model that low levels of shock wave can cause cognitive deficits in short-term learning and memory [9].

Intriguingly, epidemiological findings indicate that disruption of the blood–brain barrier (BBB) is involved in shock-wave-induced mTBI and neurological disorders such as PTSD [10]. However, such cohort studies lack the understanding of the underlying mechanisms. Thus, uncovering the molecular, biochemical, and cellular mechanisms of shock-wave–brain interactions leading to mTBI requires a careful investigation. We have shown that cerebral vascular integrity (the BBB) is very sensitive to oxidative stress during substance abuse [11,12]. Ensuing oxidative damage of the BBB leads to neuroinflammation and neuronal degeneration [13–15]. Understanding the underlying molecular and biochemical mechanisms will help us define the characteristic biomarkers of cerebral vascular injury and formulate a preventive strategy to mitigate the adverse acute effects of blast exposure and related chronic neurological complications. This includes the identification of the blast-simulated shock-wave range (shock-wave frequencies) that causes such physiological deficits and the types of mechanical or biochemical injury.

Blast injuries are classified as primary (pure blast), secondary (interaction with shrapnel or fragments), tertiary (impact with environmental structures), and/or quaternary (toxic gases) [16–18]. The 15-point Glasgow Coma Scale [19] defines severity of traumatic brain injury as mild TBI (13–15), moderate TBI (9–12), severe TBI (3–8), and vegetative state TBI (3). Mild TBI considered in this work is defined as loss of consciousness for less than 24 h [20]. At the initial stage of this study we identified the pressure range of 90–150, 150–230, and 230–350 kPa as corresponding to the mild, moderate, and severe TBI in a rodent model. All tests were conducted using a 9-in. square cross-section shock tube at the U.S. Army–University of Nebraska at Lincoln Center for Trauma Mechanics facility (Fig. 1). The detailed description of the shock-wave generator, the blast-wave spectral content, and the numerical models of skull and brain responses to blast loading and corresponding transition of blast energy are provided elsewhere [21–23]. We hypothesized that induction of oxidative stress by single (one time only shock-wave pressure exposure) and repeated (more than one shock-wave pressure exposure on the same animal) exposures to low-intensity blast overpressure initiates cerebral vascular injury (BBB damage) and neuroinflammation, which are accompanied by the release of mTBI-specific biomarkers into the blood circulation. Thus, the disruption of the barrier interface (BBB) is a key event in the acute phase of mTBI development. We demonstrate that the induction of free radical-generating enzymes, oxidative damage markers, BBB leakage, perivascular regulation by matrix metalloproteinases, and fluid channel activator aquaporin-4 ultimately leads to neuroinflammation. These pathological processes can be manifested as long-term neurological disorders.

Materials and methods

Reagents

The primary antibodies rabbit anti-NADPH oxidase 1 (NOX1), anti-inducible nitric oxide synthase (iNOS), anti-4-hydroxynonenal (4-HNE), anti-claudin-5, anti-matrix metalloproteinase 3 (MMP-3), anti-MMP-9, anti-aquaporin-4 (AQP-4), anti-Iba1, anti-caspase-3; mouse anti-GLUT1, anti-3-nitrotyrosine (3-NT), anti-MMP-2; sheep anti-von Willibrand factor (vWF); and goat anti-Iba1 were purchased from Abcam (Cambridge, MA, USA). Mouse anti-occludin antibody was purchased from Invitrogen (Carlsbad, CA, USA); rabbit anti-zonula occluden 1 (ZO-1) was from U.S. Biological (Salem, MA, USA); mouse anti-β-actin was from Millipore (Billerica, MA, USA); rabbit anti-XOX was from Santa Cruz Biotechnology (Santa Cruz, CA, USA); and mouse anti-PDGFR-β was from eBiosciences (San Diego, CA, USA). All secondary Alexa Fluor-conjugated antibodies and Fluo-3 were purchased from Invitrogen. The enzyme-linked immunosorbent assay (ELISA) kits for neuron-specific enolase (NSE) and S100β were from Alpha Diagnostic (San Antonio, TX, USA) and Abnova (Walnut, CA, USA), respectively. Evans blue (EB) and sodium fluorescein (Na-Fl) were purchased from Sigma–Aldrich (St. Louis, MO, USA).

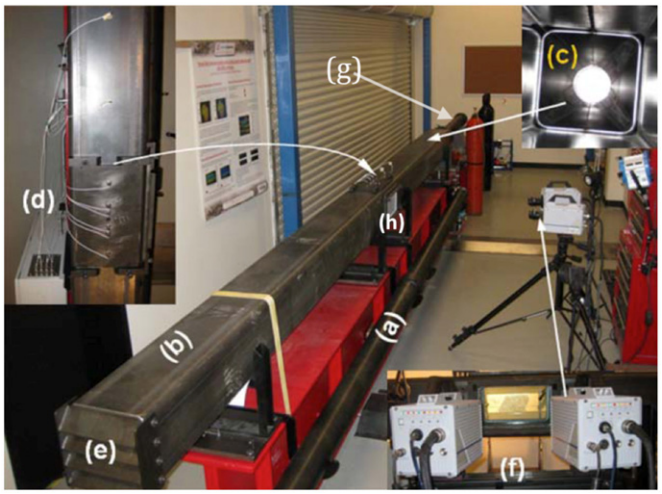

Fig. 1. Blast-wave simulation and testing facility at University of Nebraska at Lincoln. (a) 4-in. cylindrical shock tube; (b) 9-in. square shock tube; (c) transition section; (d) pressure sensor array; (e) adjustable end reflector; (f) Photron SA1.1 high-speed cameras; (g) driver section; (h) test section.

Exposure of animals to primary blast wave

Nine-week-old male Sprague–Dawley rats were purchased and maintained in sterile cages under pathogen-free conditions in accordance with the National Institutes of Health guidelines for the ethical care of laboratory animals and the Institutional Animal Care and Use Committee at the animal facility of the University of Nebraska at Lincoln. First, we determined the effects of various intensities of blasts at 123, 190, 230, and 250 kPa on the severity of brain injury. For this, we exposed 11-week-old rats (6 animals per wave intensity) to this range of blast intensities and we evaluated the blast-induced brain pathology. Second, because 123-kPa (mTBI) intensity did not cause any visible brain injury, we determined the kinetic profile of a one-time 123-kPa intensity blast on the underlying mechanisms of cerebral vascular and brain injuries at 1, 6, 24, and 48 h and 8 days postexposure in the same age group of animals (11-week-old rats). Third, after establishing the time-dependent effect at 6–24 h after 123-kPa exposure, we examined the possible exacerbating effects of repeated exposure to 123-kPa intensity at 24 h. That is, 11-week-old rats (12 rats) were exposed to 123-kPa intensity and then 24 h after the first exposure, 6 animals of the 12 were reexposed to 123-kPa intensity and left for another 24 h, which is termed here as repeated exposure or the 24 hrR group. Animals comprising the control (unexposed), 24-h exposure, and 24 hrR (6 each) groups were euthanized with a ketamine/xylazine mixture. Brain tissues were dissected out, embedded in optimal

cutting temperature compound, and kept frozen until we analyzed the mechanism of injury by immunohistochemical staining and Western blotting.

Reactive oxygen species (ROS) detection

Brain cortical tissues from the various time points of the 123-kPa blasts were washed in KDD buffer (Krebs Hepes buffer: 99 mM NaCl, 4.69 mM KCl, 2.5 mM $CaCl_2 \cdot 2H_2O$, 1.2 mM $MgSO_4 \cdot 7H_2O$, 25 mM $NaHCO_3$, 1.03 mM KH_2PO_4, 5.6 mM D-(+)-glucose, 20 mM Na–Hepes, and the chelators DF (25 μM) and DETC (5 μM)). The tissue samples were cut into small pieces with a nonmetallic (plastic) scalpel and suspended (approximately 100 mg/sample) in spin-probe solution for detection of ROS. Tissues were totally submerged in the spin-probe solution (1.0 ml) in 12-well plates before incubation at 37 °C for 30 min. Samples aspirated in a 1.0-ml syringe were snap-frozen in liquid nitrogen until detection of ROS by electron paramagnetic resonance (EPR; Bruker Escan E-box tabletop model, Serial 0264). The EPR was set at field sweep in lag time that read 10°–10 scans for an accumulative, or a "time course," protocol: microwave bridge→ attenuator 4.0 for liquid samples, 17 for frozen samples; number of scans per sample 10; hall→center field 3450.189 G, sweep width 60 G, static field 3451.189 G. We used the spin-probe solution CMH (Noxygen, NOX-2.3–100 mg; Axxora ALX-430-117-M010) in KDD buffer, which reacted with intracellular superoxide. Data are presented as cumulative detection of both the hydroxyl and the superoxide free radicals and values are expressed as amplitude of signal per milligram of tissue weight.

Immunofluorescence and microscopy

Intact external cerebral capillary vessels were surgically removed from the brain and smeared onto the slides. Adhesion and migration of Fluo-3-labeled immune cells were detected in these vessels directly under a fluorescence microscope. Brain tissue sections (8 μm thickness) containing the external and internal capillaries were used for immunofluorescence staining. Tissue sections on glass slides were washed with phosphate-buffered saline (PBS), fixed in acetone:methanol (1:1 v/v) fixative (10 min at 95 °C), and incubated for 10 min at 25 °C in 3% formaldehyde PBS. Washed tissue slides were then blocked with 3% bovine serum albumin at 25 °C for 1 h, in the absence of Triton X-100, for occludin, claudin-5, and ZO-1 staining, or in the presence of 0.1% Triton X-100 for all other antibodies, followed by overnight incubation at 4 °C with the respective primary antibodies. After being washed with PBS, the tissue slides were incubated with Alexa Fluor 488 or 594 conjugated to anti-mouse, anti-rabbit, or anti-sheep immunoglobulin G for 1 h and mounted with Immunomount containing DAPI (Invitrogen), and microphotographs were captured using a fluorescence microscope (Eclipse TE2000-U; Nikon, Melville, NY, USA).

Western blotting

Cortical brain tissues and brain microvessels were lysed with CellLytic-M (Sigma) for 30 min at 4 °C and centrifuged at 14,000*g*, and then homogenate protein concentrations were estimated using the bicinchoninic acid method (Thermo Scientific, Rockford, IL, USA). Protein load was 20 μg/lane in 4–15% sodium dodecyl sulfate–polyacrylamide gel electrophoresis (SDS–PAGE) gradient gels (Thermo Scientific). Molecular-size-separated proteins were then transferred onto nitrocellulose membranes, blocked with Superblock (Thermo Scientific), and incubated overnight with their respective primary antibodies at 4 °C, followed by incubation with horseradish peroxidase-conjugated secondary antibodies for 1 h. Immunoreactive bands were detected by West Pico chemiluminescence substrate (Thermo Scientific). Data were quantified as arbitrary densitometry intensity units using the ImageJ software package.

Zymography of MMP activity

Zymography was performed to determine MMP activities in the rat brain cortical tissue lysates using a method similar to that previously described [15]. For gelatin or casein zymography, SDS–PAGE was performed by loading 40 μg protein on a 10% polyacrylamide gel containing 0.1% gelatin or a 12% gel containing 0.1% casein (Bio-Rad, Hercules, CA, USA) at 125 V for 90 min at 4 °C. The gels were soaked in renaturing buffer (Invitrogen) for 30 min at room temperature and incubated in developing buffer (Invitrogen) for 30 min at room temperature and overnight at 37 °C. Then the gels were stained with 0.5% Coomassie Brilliant Blue R-250 in 40% methanol and 10% acetic acid for 1 h and after rinsed in distilled water. For destaining, 40% methanol and 10% acetic acid solution was used. The MMP activities showed as clear bands of lysis against a dark background of stained gelatin or casein.

Quantitative RT-PCR

Real-time quantitative PCR was performed with cDNA using the StepOnePlus Real-Time PCR System (Applied Biosystems) by employing the StepOne software version 2.0 detection system. Rat NOX1, iNOS, and glyceraldehyde-3-phosphate dehydrogenase (GAPDH) expression was analyzed using TaqMan gene expression assays and gene quantification was performed using the standard curve method as described in the software user manual. All PCR reagents and primers were obtained from Applied Biosystems and primer IDs were as follows: NOX1, Rn00583793_m1, and iNOS, Rn00586652_m1. For the endogenous control, each gene expression was normalized to that of GAPDH (Rn01775763_g1).

In vivo cell infiltration into the BBB

Rat femur bone marrow cells were isolated under sterile conditions, differentiated to monocytes with specific cell differentiating medium containing macrophage colony stimulating factor, and labeled with Fluo-3. Labeled cells were infused into the right common carotid artery (2×10^6 cells per rat) using a 27.5-gauge needle (see Alikunju et al. [13] for the detailed protocol). Adhesion and infiltration of these cells were detected in intact brain microvessels under a fluorescence microscope.

BBB permeability assay

The effect of blast exposure (123-kPa peak overpressure) on BBB permeability was examined by Na-Fl and EB tracer dye mixtures (5 μM each) using our animal model of infusion into the common carotid artery [13,24]. Two hours after the infusion of Na-Fl/EB directly into the right common carotid artery, the animals were decapitated, and the brains were removed, dissected, weighed, and homogenized in 600 μl 7.5% (w/v) trichloroacetic acid (TCA). Resulting suspensions were divided into two 300-μl aliquots. One aliquot was neutralized with 50 μl of 5 N NaOH and fluorescence was measured on a GENios microplate reader (excitation 485 nm, emission 535 nm) to determine Na-Fl concentration. The second aliquot was centrifuged for 10 min at 10,000 rpm and 4 °C, and the EB concentration in the supernatant was measured by absorbance spectroscopy at 620 nm. A standard curve was generated using serial dilutions of EB/Na-Fl solution in 7.5% TCA.

Enzyme-linked immunosorbent assay

To determine the cerebral vascular BBB leakage as well as neuronal damage by shock wave, we analyzed the neuronal- and astrocyte-specific marker proteins in blood serum samples from control rats and animals exposed to the blast with 123-kPa peak overpressure at various time points. These experiments were performed using the NSE (Alpha Diagnostic) and S100β ELISA kits (Abnova) following the manufacturer's instructions.

Terminal deoxynucleotidyl transferase dUTP nick-end labeling (TUNEL) assay

Using the TUNEL (Roche Diagnostics, Indianapolis, IN, USA) assay kit, cell apoptosis was determined in tissue sections per the manufacturer's instructions.

Data analysis

All results are expressed as the mean ± SEM. Statistical analysis of the data was performed using GraphPad Prism version 5 (Sorrento Valley, CA, USA). Comparisons between samples were performed by one-way ANOVA with Dunnett's post hoc tests. Differences were considered significant at $p < 0.05$.

Results

Determination of shock-wave range and exposure time

The objective of this study was to establish the underlying biochemical mechanisms of mTBI caused by low-frequency shock-wave exposure. To rule out the role of direct mechanical injury for development of mTBI, we determined the nature of cerebral vascular and the brain injury after exposure to frequencies of 123, 190, 230, and 250 kPa shock-wave peak overpressure. We found that there was no visible physical injury to the brain or the cerebral vasculature with the low frequencies of shock-wave exposure (Fig. 2). The higher shock waves appear to cause minor injury at the third ventricle. Based on this establishment, we determined the kinetic profile of the cerebral vascular and brain injuries at 1, 6, 24, and 48 h and 8 days postexposure in animals subjected to a single blast with 123-kPa peak overpressure. The repeated-injury scenario was tested in one group of rats exposed to 123-kPa blast twice at a 24-h interval.

Oxidative stress has a critical role in brain damage from mTBI

Initially we focused on the induction of free radical-generating enzymes, i.e., NOX1 and iNOS. Induction of these enzymes in brain microvessels was compared with the corresponding oxidative /nitrosative damage markers, 4-HNE and 3-NT. Our data indicated that at the maximum level of oxidative damage signature, 4-HNE was observed within the time frame of 6–24 h after single 123-kPa shock-wave exposure (Figs. 3A–E). However, induction of NOX1 persisted perhaps beyond 48 h and appeared to taper down at 8 days, similar to the effect seen at 1 h after the blast exposure. The mechanism of this interesting discrepancy is not understood from this study. We can only postulate that even if NOX1 induction persisted beyond 48 h, an active repair mechanism of the oxidative damage may play a role in manifesting this discrepancy. On the other hand, induction of iNOS paralleled the extent of the nitrosative damage marker 3-NT in all the time points studied, indicating a maximum increase within 6–24 h after the 123-kPa shock-wave exposure (Figs. 3A–E).

These quantitative data on the levels of the enzymes and oxidative /nitrosative damage markers were further validated by the qualitative analyses of the respective proteins and free radical-adducted markers as demonstrated by immunofluorescence staining in the brain microvessels (Fig. 4A). These data suggest that in mTBI oxidative/nitrosative stress has a critical role in the cerebrovascular inflammatory damage from a single mild TBI shock-wave exposure. Our putative conclusion was further verified by direct detection of ROS levels in the brain cortical region using EPR, which confirmed that mTBI significantly enhanced the production of ROS (Fig. 4B). We then evaluated the molecular mechanisms of mTBI-induced induction of NOX1 and iNOS by analyzing the changes in mRNA levels (transcription level) of NOX1 and iNOS using quantitative RT-PCR with TaqMan primers. Interestingly, an increase in NOX1 mRNA levels by a single 123-kPa exposure was further elevated by repeated exposure at 24 h (Fig. 4C), but there was no significant change in iNOS mRNA level (data not shown). These data suggest that upregulation of NOX1 gene expression and translational stability of its mRNA levels could be responsible for the elevation of protein levels.

Disruption of cerebral BBB and perivascular units in mTBI

After establishing the kinetics of cerebral vascular and brain injury, we then focused our study on the mechanisms of neurovascular injury, within this time frame, from single or repeated exposure. To link oxidative damage of the microvessel with that of BBB components, we examined the changes in the expression of the BBB tight-junction (TJ) proteins occludin, claudin-5, and ZO-1 by immunofluorescence staining and Western blotting. Immunofluorescence staining and microscopy analyses revealed that 123-kPa shock-wave pressure diminished the expression of TJ proteins in the microvessel within this time frame, compared with control (Fig. 5A), which is in agreement with the vascular oxidative damage results. Repeated exposure further reduced the expression of TJ proteins. These shock-wave-induced changes in TJ protein expression were validated by the alterations in the TJ protein levels after SDS–PAGE protein separation, Western blot, and quantification of the TJ protein immunoreactive bands (Figs. 5B and C).

Further, we evaluated the alterations in the BBB basement membrane component—the perivascular units that surround the TJ proteins along with the astrocyte end-feet. We used antibody to PDGFR-β as a pericyte-specific marker to detect the alterations in the perivascular structure. Both vWF and endothelial specific glucose transporter-1 (GLUT1) are authentic markers for BBB endothelium. In agreement with the disruption of TJ proteins, mild shock wave-exposed animals showed a significant reduction in PDGFR-β expression at 6 and 24 h and 24 hrR compared with controls (Fig. 6). These data suggest that disarray of perivascular units is involved in the loss of BBB integrity, neurovascular leakage,

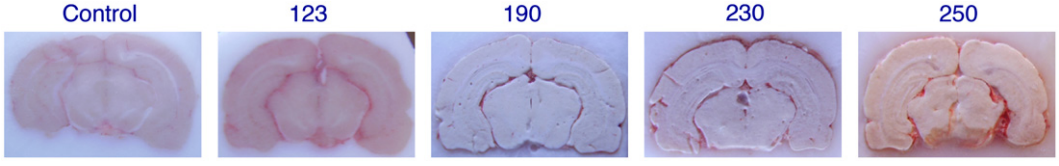

Fig. 2. Mechanical cerebrovascular injury by various blast exposures. The images show neurovascular or brain damage due to various blast exposures of mTBI, at 123, 190, 230, and 250 kPa, 24 h postexposure.

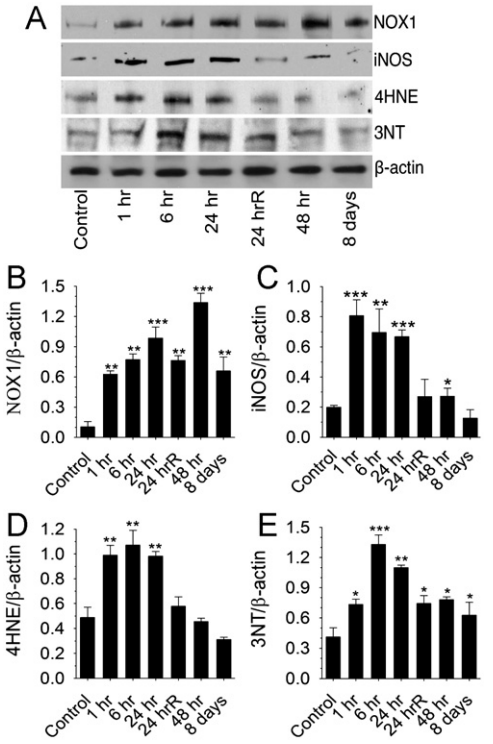

Fig. 3. mTBI induces free radical adducts in rat brain. (A) Western blot analyses of NOX1, iNOS, 4-HNE, and 3-NT in the whole rat brain homogenates at various time points after exposure to blast with 123-kPa peak. (B–E) Bar graphs show the results that are expressed as the ratio of NOX1/iNOS/4-HNE/3-NT to the β-actin band. Values are the mean ± SEM ($n=4$). $^{*}p<0.05$; $^{**}p<0.01$, $^{***}p<0.001$ versus control.

and neuroinflammatory process in primary blast mild traumatic brain injury.

Mechanistic disintegration of BBB and perivascular unit

Because activation of MMPs by oxidative stress is involved in digestion of the tight-junction and basement membrane proteins [15,25], here we examined the role of shock-wave-mediated activation of MMPs on the degradation of perivascular units and BBB leakiness. We observed that single or repeated mild shock wave exposure elevated the expression of MMP-2, MMP-3, and MMP-9 in brain microvessels (Fig. 7A). Upregulation of MMP expression was validated by significant increase in respective protein levels in brain tissue homogenates (Figs. 7B and C). We noted that the levels of MMP-3/-9 protein increased gradually up to 24 h, whereas upregulation of MMP-2 seemed to be short-lived because MMP-2 gradually decreased after 6 h. Further, detection of MMP activity by zymography validated the changes in expression and protein levels of MMPs in rat brain tissues. Thus, we found that mTBI increased the gelatinolytic (for MMP2/9) or stromelysin (for MMP3) activity in brain tissues (Fig. 7D). Taken together, these data suggest that MMP-2, MMP-3, and MMP-9 are involved in degradation of perivascular units and TJ proteins, which leads to BBB leakiness and inflammation of cerebral vascular unit.

Leakiness of cerebral vasculature due to MMP activation is often associated with the disruption of water-channel proteins. Thus, we examined the changes in AQP-4 (a water channel protein) and the development of edema around the vasculature. Indeed, enhanced expression of AQP-4 was observed around the perivascular region and within cortical brain tissue of mTBI animals (Fig. 8A). We then established the cell phenotypes that are associated with brain edema

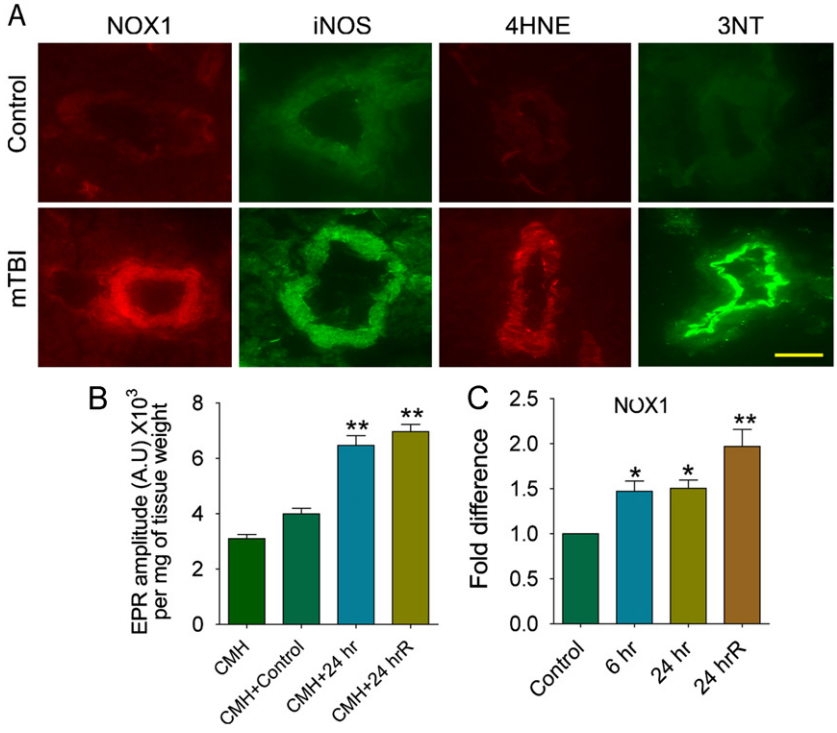

Fig. 4. Primary blast induced oxidative and nitrosative stress in the rat brain microvessels. (A) Immunofluorescent staining of NOX1, iNOS, 4-HNE, and 3-NT in intact brain microvessels of rats subjected to a single blast with 123-kPa peak overpressure, 24 h postexposure. (B) ROS generation was detected by EPR in brain tissue slices from mTBI 24 h and 24 hrR postexposure to 123-kPa blast and compared with control. Results are expressed in EPR amplitude arbitrary units per milligrams of tissue weight. (C) Changes in mRNA level of NOX1 in brain cortical tissues of rats at different time intervals postexposure to 123-kPa blast by quantitative RT-PCR using TaqMan primers. Values are the mean ± SEM ($n=3$ in (B) and (C)). Statistically significant, $^{*}p<0.05$, $^{**}p<0.01$ versus control in (C) and versus CMH + control in (B). Scale bar in (A), 5 μm.

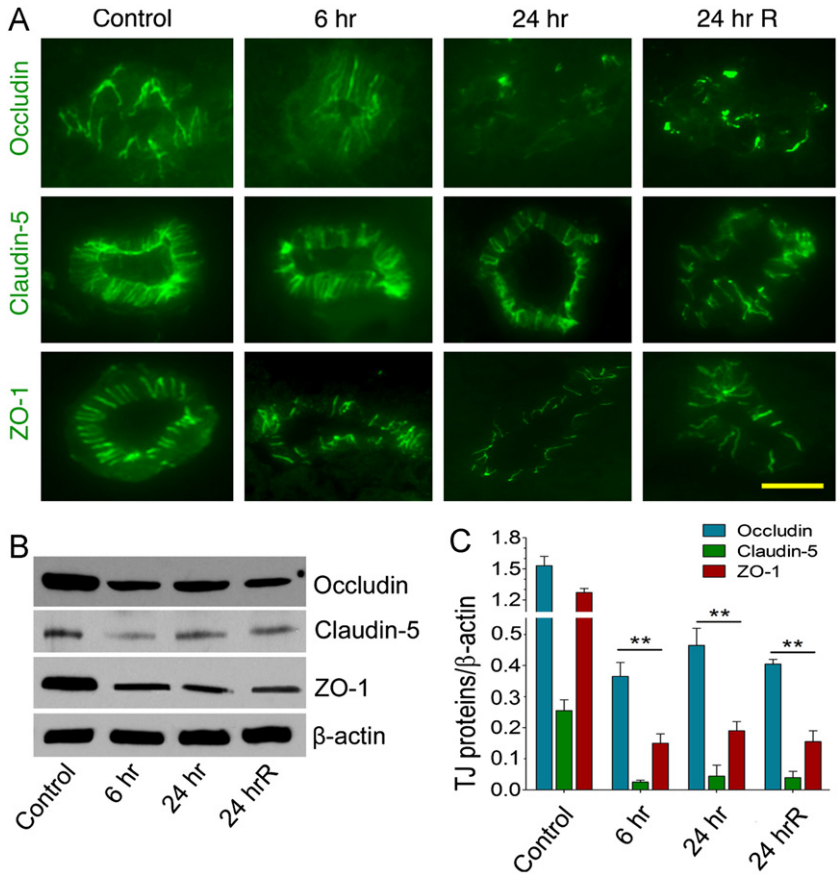

Fig. 5. Primary blast causes impairment in tight-junction proteins. (A) Immunofluorescent staining of tight-junction proteins occludin, claudin-5, and ZO-1 in intact brain microvessels of rats at different times postexposure (blast with 123-kPa peak overpressure): 6 h, 24 h, and 24 hrR (two repeated exposures 24 h apart). (B) Western blot analysis of occludin, claudin-5, ZO-1, and actin in the whole brain tissue homogenates of rats at different times after exposure to blast (123-kPa peak overpressure). (C) Graph shows the results that are expressed as the ratio of occludin/claudin5/ZO-1 to the β-actin band. Values are the mean ± SEM ($n=3$). Statistically significant, $^{**}p<0.01$ versus control in (C). Scale bar in (A), 5 μm.

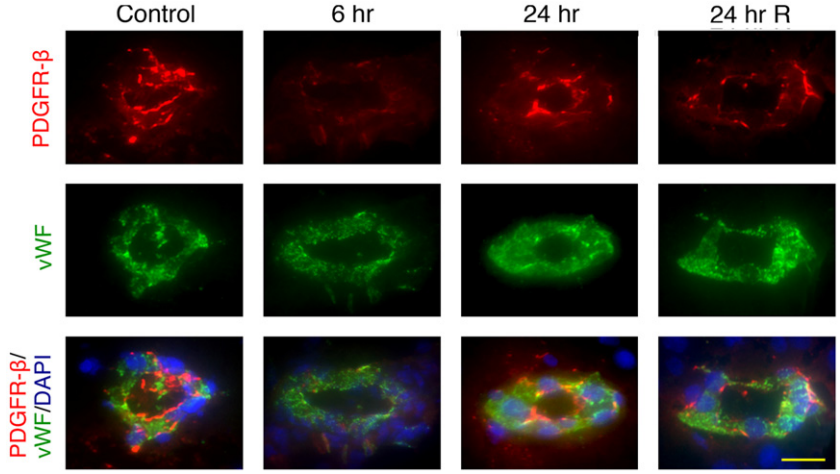

Fig. 6. Pericytes have significant role in BBB dysfunction in primary blast-induced mTBI. Immunofluorescent staining of the pericyte-specific marker PDGFR-β (red) and endothelial marker vWF (green) in intact brain microvessels of rats exposed to primary blast (123-kPa peak overpressure). Cell nuclei were counterstained with DAPI (blue). The expression of PDGFR-β decreased with time (6 and 24 h, single exposure) and after repeated insult (24 hrR). Scale bar, 5 μm.

formation around the perivascular unit. To achieve this we colocalized AQP-4 with the astrocyte marker glial fibrillary acidic protein (GFAP) or with the microglia marker ionized calcium-binding adaptor molecule 1 (Iba1) in brain tissue cross sections (8 μm thick) and detected them by immunofluorescent staining using specific antibodies to the respective protein markers. Our data showed that AQP-4 water channel activation in mTBI was associated with astrocytes, most likely toward the astrocyte end-feet surrounding the perivascular region (Fig. 8B). We failed to observe any significant colocalization of AQP-4 and the microglia marker Iba1 in the brain

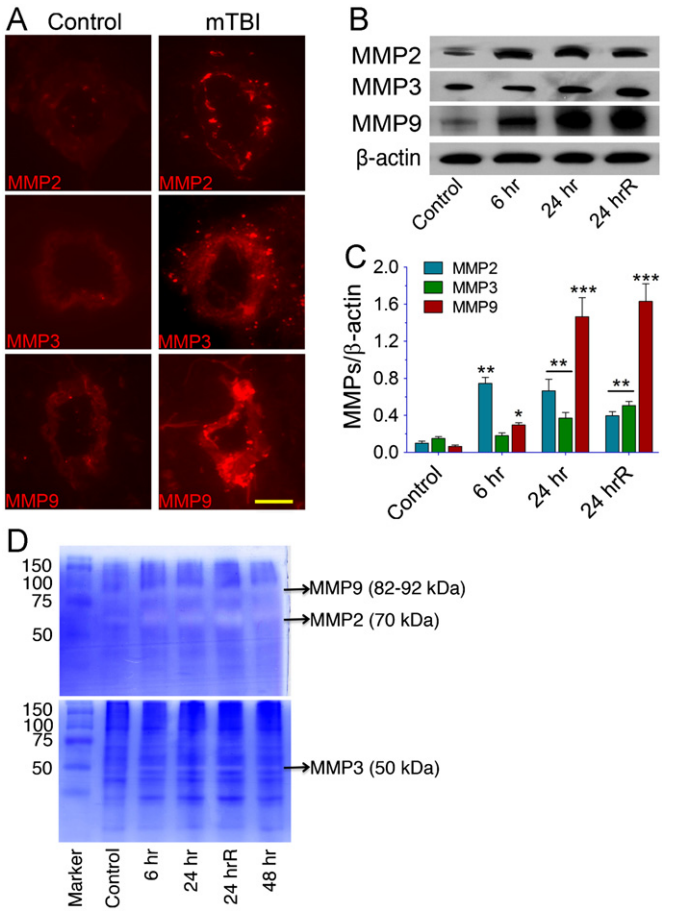

Fig. 7. mTBI activates matrix metalloproteinases (MMPs). (A) Immunofluorescent staining of MMP-2, MMP-3, and MMP-9 in intact brain microvessels of mTBI-exposed and control rats. (B) Western blot analyses of MMP-2, MMP-3, MMP-9, and actin in whole brain tissue homogenates. (C) Graph shows the results expressed as the ratio of MMP-2/3/9 to the β-actin band. (D) The gelatinolytic activity of MMP-2/9 (top gel) and caseinolytic activity of MMP-3 (bottom gel) were demonstrated by gelatin or casein zymography in the rat brain cortical tissue protein extracts from various time periods, 6 h, 24 h, 24 hrR, and 48 h, after exposure to blast with 123-kPa peak overpressure. Values are the mean ± SEM; $n=4$. Statistically significant, $^{**}p<0.01$, $^{***}p<0.001$, versus control in (C). Scale bar in (A), 5 μm.

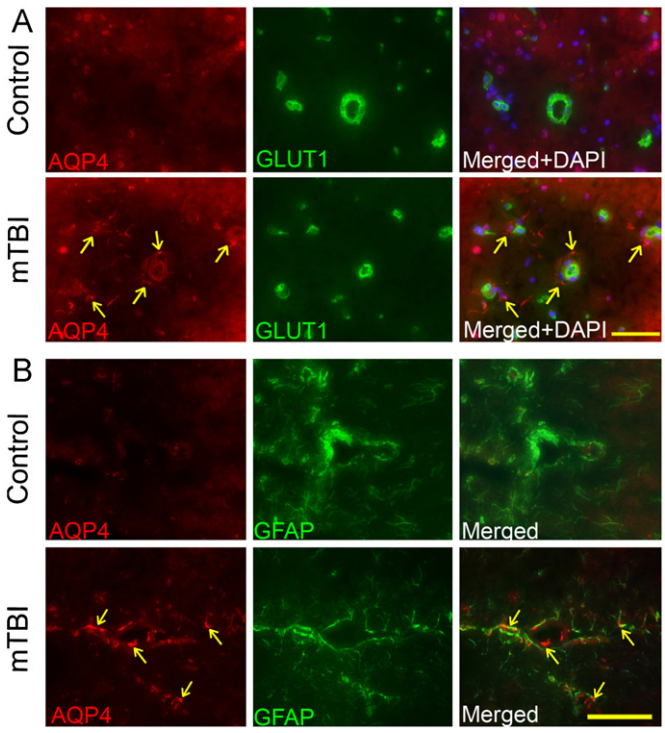

Fig. 8. mTBI activates aquaporin-4. (A) Immunofluorescent staining of AQP-4 (red) and the endothelial marker GLUT1 (green) in brain tissue sections containing microvessels exposed to primary blast (123-kPa peak overpressure). Cell nuclei were counterstained with DAPI (blue). The arrows indicate the AQP-4 staining surrounding the microvessels. Scale bar, 40 μm. (B) Immunofluorescent staining of AQP-4 (red) colocalized with GFAP (astrocyte marker, green) in brain tissue sections containing microvessels exposed to primary blast (123-kPa peak overpressure). The arrows indicate the AQP-4 staining surrounding the microvessels. Scale bar, 40 μm.

region (data not shown). This result suggests that cerebrovascular edema formation by AQP-4 activation may promote vascular fluid cavitation and neuroinflammation in blast-induced mild traumatic brain injury.

Assessment of cerebral vascular (BBB) leakage

Disruption of cerebral vascular barrier integrity as a result of TJ protein damage and perivascular cavitation was assessed by leaking in and leaking out of biomarkers across the BBB. Infiltration of immune cells into the brain was assayed by adhesion and migration of Fluo-3-labeled macrophages, and the permeativity of Na-Fl/EB tracers across the BBB assessed the tightness of the vasculature. Leaking out of brain matter into the blood circulation after shock wave exposure was analyzed by detecting S100β and NSE in blood samples, which are commonly used in traumatic brain injury events [26]. We observed that adhesion/infiltration of Fluo-3-labeled cells was significantly enhanced in the microvessels of mTBI shock-wave-exposed animals compared with controls (Fig. 9A). Adhesion and infiltration of these immune cells appeared to occur at the vascular injury sites. Similarly, mTBI shock wave exposure greatly increased the permeativity of small-molecular-weight Na-Fl (MW 376) and high-molecular-weight-tracer EB (MW 961) across the BBB compared with respective controls (Fig. 9B), which correlated with the enhanced immune cell adhesion and infiltration into the brain. Intriguingly, mTBI shock wave-exposed animals also showed significantly higher levels of S100β and NSE in the blood samples compared with controls (Fig. 9C). The maximum level of S100β was found at 6 h, whereas leaking of NSE across the damaged BBB into the bloodstream continued to increase even at 24 h after the primary blasts. The elevation of S100β and NSE in the plasma of mTBI animals clearly indicated that degenerated/injured glial/neuronal cell body contents were leaked out of the brain and into the circulation. These data also supported the findings that activated caspase-3- and TUNEL-positive cells observed in the brain could well be degenerated neurons and glial cells.

Vascular injury and inflammation lead to neurovascular cell apoptosis

To correlate oxidative injury and inflammation with possible cell death around the cerebral vasculature, we then examined the activation of the caspase-3 intrinsic apoptotic pathway in brain tissue sections in the control and shock wave experimental conditions. We also used GLUT1 as a positive marker for brain endothelium (BBB). It was obvious that brain microvessels and brain tissue from 123-kPa shock-wave exposure showed much higher expression of caspase-3 protein than those of controls (Fig. 10A). Western blot analyses further substantiated the significant increase in caspase-3 protein levels in rat brain tissue homogenates of either single or repeated exposure to blast wave compared with controls (Fig. 10B). As expected, repeated blast resulted in an increase in caspase-3 expression that was higher than the single exposure.

To validate the activation of caspase-3, we evaluated cell apoptosis by TUNEL, and we confirmed that TUNEL-positive cell

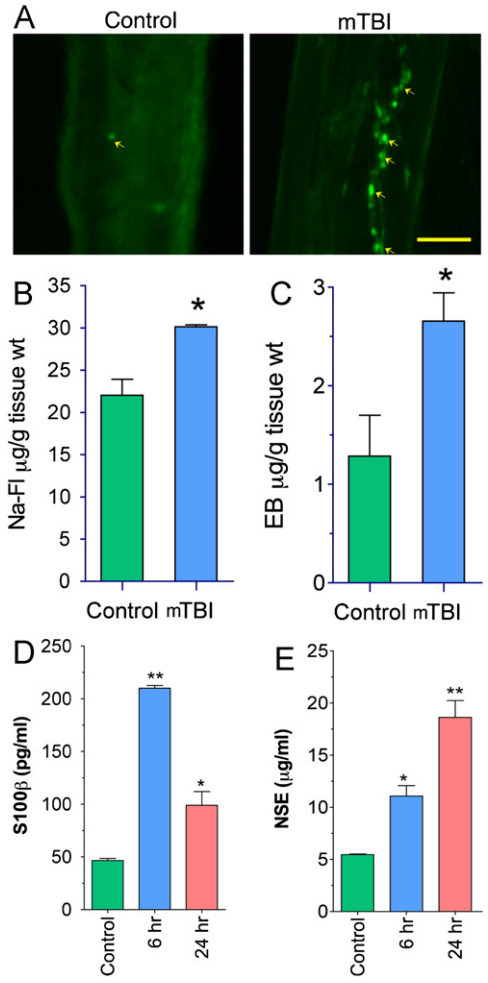

Fig. 9. mTBI causes BBB leakage. (A) Fluo-3-labeled macrophage adhesion/migration in brain capillary after infusion of cells into the common carotid artery of mTBI-exposed rats 24 h after the blast compared with controls. (B, C) Graphical representation of in vivo permeability to show the leakage of (B) Evans blue (EB; 5 μM) and (C) sodium fluorescein (Na-Fl; 5 μM) in mTBI-exposed rats. The carotid artery of rats was exposed and infused with EB/Na-Fl mixture and the brain was collected after 1 h of infusion and processed for BBB permeability assay as given under Materials and methods. (D, E) ELISA shows the levels of (D) S100β and (E) NSE in the blood serum of mTBI-exposed rats. The blood serum was collected 24 h after blast exposure. Values are the mean ± SEM, $n=3$ in (B) and (C) and $n=5$ in (D) and (E). $^{*}p<0.05$, $^{**}p<0.01$, statistically significant in (B–E). Scale bar in (A), 40 μm.

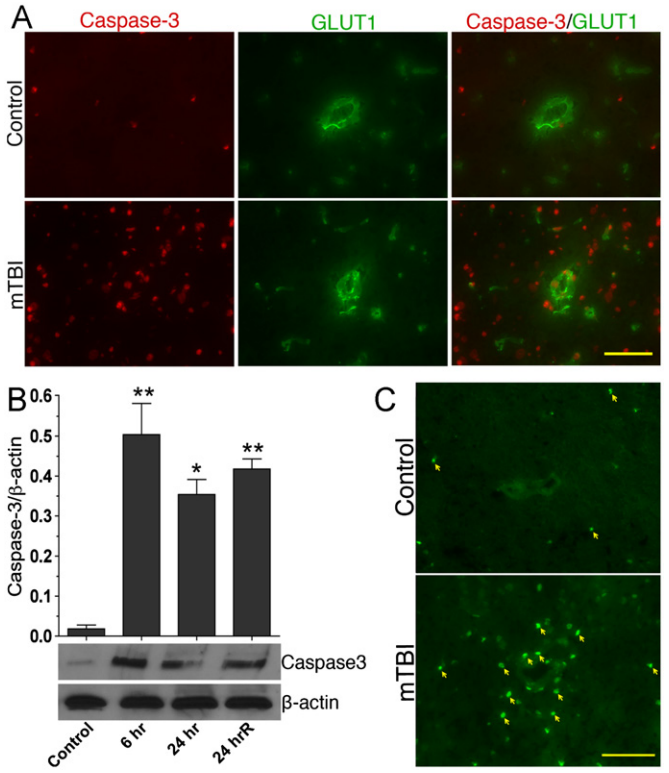

Fig. 10. mTBI causes cell apoptosis. (A) Changes in the expression of active caspase-3 (red) in brain microvessels and cortical tissue sections of control and mTBI blast (123 kPa)-exposed animals. (B) Immunoblot analysis to show the alterations in active caspase-3 protein levels in brain cortical tissue and microvessel homogenate proteins. Bar graph shows the results, which are expressed as ratio of caspase-3 (active) to β-actin bands. Values are the mean ± SEM; $n=4$ or 5. $^{*}p<0.05$, $^{**}p<0.01$, statistically significant. (C) TUNEL staining in rat brain cortical tissue section. The arrows indicate the TUNEL-positive cells. Scale bar in (A) and (C), 20 μm.

numbers were much higher in the brain tissue exposed to blast wave than in the control, similar to the caspase-3 activation data (Fig. 10C). The activation of caspase-3 and TUNEL positivity in cells were not confined to the cerebral vascular but appeared to spread throughout the brain parenchyma in mTBI. Taken together, these results clearly indicate that oxidative injury of the BBB by mTBI shock wave pressure causes vascular edema, BBB leakage, and neurovascular inflammation and degeneration.

Discussion

To the best of our knowledge, the present findings are the first to describe the mechanisms of cerebral vascular damage by shock wave in mTBI exposure. We established that low-frequency shock wave pressure causes biochemical cerebral vascular/brain injury, which occurs within a window of 6–24 h after the exposure. The nature of vascular injury is oxidative damage and inflammation, which is initiated by oxidative/nitrosative reactive stress via the induction of NOX1 and iNOS by blast wave. The signature of oxidative damage (4-HNE) and nitrated protein (3-NT) in the microvessels paralleled an induction of NOX1/iNOS and its kinetic profile. Based on these findings, it is apparent that any neurovascular inflammation and neuronal degeneration are expected to occur within this time frame after single shock wave exposure in animal model. Thus, in a single mild shock wave exposure, one can miss the cerebral vascular injury and neuropathological signature outside this time frame, because oxidative injury and inflammatory response gradually diminish after 24 h. A constant counteracting injury repair process (wound healing process) operating in a dynamic self-organizing system of the tissue organ may account for the disappearance of the vascular injury after 24 h. This brings up the vital issue of experimental design, in that a single low shock wave intensity in an animal model may not be ideal for the investigation of long-term neurocognitive deficits, behavioral changes, and neurological disorders such as PTSD. A repeated exposure to mild primary blasts is suggested for such type of neurocognitive and behavioral studies, which is demonstrated here by a prolonged vascular damage from repeated primary blast exposures.

It may be noted here that there are dramatic changes at 24 h from a single 123-kPa blast and a delayed onset of effects of repeated blast exposure on the outcome of oxidative markers. This is also manifested by the reversibility of the effects of a single primary blast wave and the prolonged effect of repeated blasts that is not easily reversible. These acute dramatic changes and delayed-onset effects may influence the pathological signature of the single and repeated blast-wave brain injury and the outcome of cognitive behavior changes in long-term exposure to primary blasts. We are currently investigating the significance of these acute dramatic and delayed-onset effects of

single and repeated exposure to blast wave in relation to the outcome of cognitive behavior changes.

It is evident from this study that mild shock wave causes cerebral vascular injury; thus, moderate to severe shock wave primary blast intensity is expected to exacerbate cerebral vascular injury. Here we demonstrate the pathophysiological evidence that disruption of the BBB and perivascular components by primary blast wave pressure contributes to neuroinflammation and neurotrauma. The association of cerebral vascular oxidative injury with a concomitant reduction in the BBB TJ proteins and the perivascular units with subsequent enhanced immune cell infiltration justified the notion that vascular barrier breakdown precedes neuroinflammation. Loosening of this barrier interface by shock-wave exposure is mediated by oxidative stress-induced MMPs and fluid channel aquaporin-4 activation in the perivascular units. The pericyte is an integral unit of the neurovascular components that contributes to the integrity of the BBB, and destruction of this barrier leads to neurodegenerative disease [27,28]. Our findings suggest that degradation of the TJ proteins and perivascular units by MMPs promotes BBB leakiness, vascular fluid cavitation, edema formation, and neuroinflammation.

In the context of these findings, we can emphasize that cerebral vascular oxidative injury and inflammation may precede the development of blast-induced neurotrauma. This claim is substantiated by the fact that there was a strong association between vascular BBB damage and neuronal-specific protein leakage into the bloodstream. Leakage of brain matter from the cerebrospinal fluid into the blood circulation is possible only if the BBB function is impaired and brain cells (neurons, astrocytes) in the proximity of the perivascular area are either injured or dead. This close proximity to the BBB may also explain why the levels of S100β in plasma rose much faster (6 h) than those of NSE (24 h) after mTBI exposure as demonstrated in these studies. Indeed, our findings validated that caspase-3 activation and cell apoptosis (TUNEL-positive cells) were observed mostly around the perivascular region of the brain. Our concept of cerebral vascular injury occurring before neurotrauma and neurological disease in single or repeated shock-wave exposure is strongly supported by the recent findings of Goldstein et al. [29]. In this neurotrauma mouse model of primary blast, the authors demonstrated an impressive neurodegeneration in the form of phosphorylated tau protein clearly localized around the perivascular region. This distinctive localization of tauopathy surrounding the perivascular region lends evidence that vascular BBB oxidative injury/inflammation paves the way for neuroinflammation and neuronal degeneration within the neurovascular layers. This interconnected event is functionally demonstrated in the present studies by the detection of biochemical and pathological biomarkers with evidence of enhanced BBB permeability (Na-Fl/EB tracers), neuroinflammation (increase in infiltration of immune cells), and neuroastroglial degeneration as evident by the elevated leakage of NSE/S100β into the bloodstream. We conclude that induction of oxidative stress and subsequent MMP activation by shock-wave pressure lead to cerebral vascular BBB leakage, vascular edema formation, neuroinflammation, and neurodegeneration.

Acknowledgments

This work was supported by NIH/NIAAA Grants R21 AA020370-01A1 and RO1 AA017398 to J.H. and by the U.S. Army Research Office project “Army–UNL Center of Trauma Mechanics” (Contract W911NF- 08-10483) to N.C.

References

[1] Hoge, C. W.; McGurk, D.; Thomas, J. L.; Cox, A. L.; Engel, C. C.; Castro, C. A. Mild traumatic brain injury in U.S. soldiers returning from Iraq. *N. Engl. J. Med.* **358:**453–463; 2008.

[2] Vanderploeg, R. D.; Belanger, H. G.; Horner, R. D.; Spehar, A. M.; Powell-Cope, G.; Luther, S. L.; Scott, S. G. Health outcomes associated with military deployment: mild traumatic brain injury, blast, trauma, and combat associations in the Florida National Guard. *Arch. Phys. Med. Rehabil.* **93:**1887–1895; 2012.

[3] Vasterling, J. J.; Verfaellie, M.; Sullivan, K. D. Mild traumatic brain injury and posttraumatic stress disorder in returning veterans: perspectives from cognitive neuroscience. *Clin. Psychol. Rev.* **29:**674–684; 2009.

[4] Trudeau, D. L.; Anderson, J.; Hansen, L. M.; Shagalov, D. N.; Schmoller, J.; Nugent, S.; Barton, S. Findings of mild traumatic brain injury in combat veterans with PTSD and a history of blast concussion. *J. Neuropsychiatry Clin. Neurosci* **10:**308–313; 1998.

[5] Santiago, P. N.; Wilk, J. E.; Milliken, C. S.; Castro, C. A.; Engel, C. C.; Hoge, C. W. Screening for alcohol misuse and alcohol-related behaviors among combat veterans. *Psychiatr. Serv.* **61:**575–581; 2010.

[6] Wilk, J. E.; Bliese, P. D.; Kim, P. Y.; Thomas, J. L.; McGurk, D.; Hoge, C. W. Relationship of combat experiences to alcohol misuse among U.S. soldiers returning from the Iraq war. *Drug Alcohol Depend.* **108:**115–121; 2010.

[7] Otis, J. D.; McGlinchey, R.; Vasterling, J. J.; Kerns, R. D. Complicating factors associated with mild traumatic brain injury: impact on pain and posttraumatic stress disorder treatment. *J. Clin. Psychol. Med. Settings* **18:**145–154; 2011.

[8] Kamnaksh, A.; Kovesdi, E.; Kwon, S. K.; Wingo, D.; Ahmed, F.; Grunberg, N. E.; Long, J.; Agoston, D. V. Factors affecting blast traumatic brain injury. *J. Neurotrauma* **28:**2145–2153; 2011.

[9] Vandevord, P. J.; Bolander, R.; Sajja, V. S.; Hay, K.; Bir, C. A. Mild neurotrauma indicates a range-specific pressure response to low level shock wave exposure. *Ann. Biomed. Eng.* **40:**227–236; 2012.

[10] Higashida, T.; Kreipke, C. W.; Rafols, J. A.; Peng, C.; Schafer, S.; Schafer, P.; Ding, J. Y.; Dornbos, D. 3rd; Li, X.; Guthikonda, M.; Rossi, N. F.; Ding, Y. The role of hypoxia-inducible factor-1alpha, aquaporin-4, and matrix metalloproteinase-9 in blood–brain barrier disruption and brain edema after traumatic brain injury. *J. Neurosurg.* **114:**92–101; 2011.

[11] Haorah, J.; Floreani, N. A.; Knipe, B.; Persidsky, Y. Stabilization of superoxide dismutase by acetyl-l-carnitine in human brain endothelium during alcohol exposure: novel protective approach. *Free Radic. Biol. Med.* **51:**1601–1609; 2011.

[12] Rump, T. J.; Abdul Muneer, P. M.; Szlachetka, A. M.; Lamb, A.; Haorei, C.; Alikunju, S.; Xiong, H.; Keblesh, J.; Liu, J.; Zimmerman, M. C.; Jones, J.; Donohue Jr T. M.; Persidsky, Y.; Haorah, J. Acetyl-l-carnitine protects neuronal function from alcohol-induced oxidative damage in the brain. *Free Radic. Biol. Med.* **49:**1494–1504; 2010.

[13] Alikunju, S.; Abdul Muneer, P. M.; Zhang, Y.; Szlachetka, A. M.; Haorah, J. The inflammatory footprints of alcohol-induced oxidative damage in neurovascular components. *Brain Behav. Immun.* **25(Suppl. 1):**S129–S136; 2011.

[14] Haorah, J.; Ramirez, S. H.; Floreani, N.; Gorantla, S.; Morsey, B.; Persidsky, Y. Mechanism of alcohol-induced oxidative stress and neuronal injury. *Free Radic. Biol. Med.* **45:**1542–1550; 2008.

[15] Abdul Muneer, P. M.; Alikunju, S.; Szlachetka, A. M.; Haorah, J. The mechanisms of cerebral vascular dysfunction and neuroinflammation by MMP-mediated degradation of VEGFR-2 in alcohol ingestion. *Arterioscler. Thromb. Vasc. Biol.* **32:**1167–1177; 2012.

[16] DePalma, R. G.; Burris, D. G.; Champion, H. R.; Hodgson, M. J. Blast injuries. *N. Engl. J. Med.* **352:**1335–1342; 2005.

[17] Moore, D. F.; Radovitzky, R. A.; Shupenko, L.; Klinoff, A.; Jaffee, M. S.; Rosen, J. M. Blast physics and central nervous system injury. *Future Neurol* **3:**243–250; 2008.

[18] Chen, Y. C.; Smith, D. H.; Meaney, D. F. In-vitro approaches for studying blast-induced traumatic brain injury. *J. Neurotrauma* **26:**861–876; 2009.

[19] Teasdale, G.; Jennett, B. Assessment of coma and impaired consciousness: a practical scale. *Lancet* **2:**81–84; 1974.

[20] Okie, S. Traumatic brain injury in the war zone. *N. Engl. J. Med.* **352:**2043–-2047; 2005.

[21] Chandra, N.; Holmberg, A.; Feng, R. Controlling the shape of the shock wave profile in a blast facility. U.S. Provisional Patent Application No. 61542354, 3 October 2011.

[22] Ganpule, S.; Alai, A.; Plougonven, E.; Chandra, N. Mechanics of blast loading on the head: models in the study of traumatic brain injury using experimental and computational approaches. Biomech. Model. Mechanobiol. (in press).

[23] Sundaramurthy, A.; Alai, A.; Ganpule, S.; Holmberg, A.; Plougonven, E.; Chandra, N. Blast-induced biomechanical loading of the rat: an experimental and anatomically accurate computational blast injury model. *J. Neurotrauma* **29:**2352–2364; 2012.

[24] Abdul Muneer, P. M.; Alikunju, S.; Szlachetka, A. M.; Murrin, L. C.; Haorah, J. Impairment of brain endothelial glucose transporter by methamphetamine causes blood–brain barrier dysfunction. *Mol. Neurodegener* **6:**23; 2011.

[25] Haorah, J.; Schall, K.; Ramirez, S. H.; Persidsky, Y. Activation of protein tyrosine kinases and matrix metalloproteinases causes blood–brain barrier injury: novel mechanism for neurodegeneration associated with alcohol abuse. *Glia* **56:**78–88; 2008.

[26] Berger, R. P.; Adelson, P. D.; Pierce, M. C.; Dulani, T.; Cassidy, L. D.; Kochanek, P. M. Serum neuron-specific enolase, S100B, and myelin basic protein concentrations after inflicted and noninflicted traumatic brain injury in children. *J. Neurosurg.* **103:**61–68; 2005.

[27] Winkler, E. A.; Bell, R. D.; Zlokovic, B. V. Central nervous system pericytes in health and disease. *Nat. Neurosci.* **14:**1398–1405; 2011.

[28] Daneman, R.; Zhou, L.; Kebede, A. A.; Barres, B. A. Pericytes are required for blood–brain barrier integrity during embryogenesis. *Nature* **468:**562–566; 2010.

[29] Goldstein, L. E.; Fisher, A. M.; Tagge, C. A.; Zhang, X. L.; Velisek, L.; Sullivan, J. A.; Upreti, C.; Kracht, J. M.; Ericsson, M.; Wojnarowicz, M. W.; Goletiani, C. J.; Maglakelidze, G. M.; Casey, N.; Moncaster, J. A.; Minaeva, O.; Moir, R. D.; Nowinski, T.; Stern, R. A.; Cantu, R. C.; Geiling, J.; Blusztajn, J. K.; Wolozin, B. L.; Ikezu, T.; Stein, T. D.; Budson, A. E.; Kowall, N. W.; Chargin, D.; Sharon, A.; Saman, S.; Hall, G. F.; Moss, W. C.; Cleveland, R. O.; Tanzi, R. E.; Stanton, P. K.; McKee, A. C. Chronic traumatic encephalopathy in blast-exposed military veterans and a blast neurotrauma mouse model. *Sci. Transl. Med.* :134ra160; 2012.